Published in final edited form as:
Environ Sci Technol. 2011 January 15; 45(2): 719–725. doi:10.1021/es102420r.

Recovery of Phenanthrene-Degrading Bacteria After Simulated *In Situ* Persulfate Oxidation in Contaminated Soil

Stephen D. Richardson[†], **Benjamin L. Lebron**[‡], **Cass T. Miller**, and **Michael D. Aitken**[*]
Department of Environmental Sciences and Engineering Gillings School of Global Public Health University of North Carolina at Chapel Hill

Abstract

A continuous-flow column study was conducted to investigate the long-term effects of persulfate oxidation on the abundance and activity of the indigenous microbial community and phenanthrene-degrading bacteria in contaminated soil from a former manufactured gas plant (MGP) site. Approximately six pore volumes of a 20 g/L persulfate solution were introduced into the column, followed by simulated groundwater for 500 d. Soil samples were collected from the surface of the soil bed and along the column length immediately before and after persulfate injection and up to 500 d following injection. Exposure to persulfate led to a two- to three-log reduction in total bacterial 16S rRNA genes, severe inhibition of ^{14}C-acetate mineralization (as a measure of general microbial activity), and a decrease in community diversity. However, relatively rapid recovery of both bacterial gene abundance and activity was observed within 30 d after persulfate exposure. Mineralization of ^{14}C-phenanthrene was also inhibited but did not recover until 100 d post-oxidation. Known phenanthrene-degrading bacterial groups decreased to below detection limits throughout the column, with recovery times from 100 d to 500 d after persulfate injection. These findings suggest that coupling biological processes with persulfate oxidation is possible, although recovery of specific contaminant degraders may occur much later than the general microbial community recovers. Furthermore, the use of total bacterial quantity or non-specific measures of activity as a surrogate for the recovery of contaminant degraders may be inappropriate for evaluating the compatibility of chemical treatment with subsequent bioremediation.

Introduction

Implementation of *in situ* chemical oxidation (ISCO) as the sole treatment strategy at contaminated field sites often does not decrease contaminant concentrations below regulatory guidelines, despite successful oxidation and transformation of large portions of the contaminant mass (1,2). Insufficient oxidant delivery due to soil matrix heterogeneities, high oxidant reactivity with soil organic matter (SOM), and/or gas production can leave zones of residual contamination post-oxidation. Contaminant rebound, a phenomenon governed by slow mass transfer of contaminants from these residual zones, is generally responsible for continued long-term groundwater contamination after oxidant depletion (3,4). Secondary treatment strategies such as natural attenuation or enhanced bioremediation can play an important role in reducing residual contaminant concentrations and may prove beneficial in a combined remediation scenario. The goal in a combined or staged

[*] Corresponding author: phone 919-966-1024; mike_aitken@unc.edu.
[†]Currently at: Solutions-IES, Inc.
[‡]Currently at: CH2M-Hill

Brief: Phenanthrene-degrading bacteria recovered much later than the general microbial community following *in situ* chemical oxidation with persulfate in field-contaminated soil.

remediation effort is to remove the bulk of the contaminant mass using aggressive treatments (such as ISCO), while allowing biological processes to serve as a "polishing" step for remediation of residual contaminant mass (2,5).

Coupling of ISCO and bioremediation is complicated by the effects of oxidant exposure on the indigenous microbial community. Chemical oxidation can impact the activity and growth of microbes by changing conditions in the subsurface, such as the availability of an electron acceptor or substrate, temperature, and pH (3,6). Oxidants and their reactive species can also be highly toxic to microorganisms, directly attacking a variety of cellular components (4,7,8).

Studies investigating the effects of ISCO on biological processes have focused primarily on Fenton's reagent (9-13) and permanganate (1,2,14-16) for the oxidation of chlorinated aliphatic hydrocarbons and, to a lesser extent, polycyclic aromatic hydrocarbons (PAHs) in spiked and field-contaminated soils. In the majority of previous studies, complete recovery or enhancement of the overall microbial community was observed post-oxidation, in most cases within six months of oxidant exposure. Few studies, however, have investigated the effects of oxidant addition on specific contaminant-degrading microorganisms.

Persulfate is the newest and least-studied of the available oxidants, only recently receiving attention as an alternative oxidant for soil and groundwater remediation (17). The aqueous decomposition of persulfate anion ($S_2O_8^{2-}$) can be initiated by heat activation (in addition to base, peroxide, and transition-metal catalysis) to form sulfate radicals ($SO_4^{-\bullet}$) (18-20), which react with a wide range of environmental contaminants (3), including PAHs (21-23). In soil, the resulting sulfate radicals are free to react with available contaminants, SOM, and microorganisms, and they can form other reactive species such as the hydroxyl radical ($OH^{\bullet}$), peroxymonosulfate (HSO_5^-), and hydrogen peroxide (H_2O_2) (24,25). Subsequent reactions involving $OH^{\bullet}$ and H_2O_2 can yield molecular oxygen (19,20), although other reactions of these active oxygen species are likely to occur in soil as well.

Only one peer-reviewed study has examined the effects of persulfate on indigenous soil microorganisms. Tsitonaki et al. (26) exposed leachate-contaminated aquifer material to various doses of persulfate (0.02-2 g/kg) at 40°C and monitored changes in cell density and activity of the indigenous community using a standard viability assay and ^{14}C-acetate mineralization, respectively. To our knowledge, no study has investigated the effects of persulfate on specific PAH-degrading bacteria and tracked their long-term recovery post-oxidation in field-contaminated soil. We used cultivation-independent techniques to measure the quantity and activity of the total bacterial community and known phenanthrene-degrading bacteria in response to the injection of persulfate in a laboratory column packed with contaminated soil from a former manufactured gas plant (MGP) site. We focused on phenanthrene because it was the most predominant PAH in the soil.

Materials and Methods

Chemicals

Dichloromethane (>99.5%), acetone (>99.5%), acetonitrile (>99.9%), sodium sulfate (>99%), and sodium persulfate (>98%) were purchased from Fisher Scientific Inc. (Pittsburgh, PA). Anthracene-d_{10} (98%) was purchased from Cambridge Isotope Laboratories (Andover, MA). [U-^{14}C] sodium acetate (97.1%; 56 mCi/mmol in ethanol) and [9-^{14}C] phenanthrene (>98%; 8.3 mCi/mmol in methanol) were purchased from Sigma-Aldrich (St. Louis, MO).

Soil

Contaminated soil was collected from a former MGP site in Salisbury, NC, USA. The soil was sieved through a 10-mm wire screen, mixed with sterile 40/50 grade silica sand (Unimin Corporation, Le Sueur, MN) at a 50:50 ratio (dry weight), and stored at 4°C prior to column packing. Addition of the silica sand was necessary to maintain low-pressure flow during long-term column operation; preliminary column studies with the source material yielded very high inlet pressures (>100 psi). Sand addition had minimal impact on the indigenous soil microbial community as evaluated by denaturing-gradient gel electrophoresis (DGGE; data not shown). In subsequent discussion, the final packing material is referred to as "column soil".

The column soil contained 83% sand, 14% silt, and 3% clay, with total organic matter of 8.3% as determined by a thermogravimetric method (27) and extractable organic matter of 0.64%. The total concentration of the PAHs analyzed was 295 ± 65 mg/kg dry soil (n = 33), with phenanthrene comprising 44% of the total PAH mass (129 ± 31 mg/kg). A complete list of physical properties and PAH concentrations for the column soil is presented in the Supporting Information (Tables S1 - S3).

Simulated Groundwater

Simulated groundwater was prepared based on historical ion concentrations of groundwater in the region of the MGP site (28). The solution contained 1.83 g $CaCl_2 \cdot H_2O$, 1.01 g $MgSO_4 \cdot 7H_2O$, 2.19 g $NaHCO_3$, 1 ml of an 88 mg/L KCl solution, and 1 ml of 1 N H_2SO_4 in 20 L of sterile-filtered reagent water. New batches of groundwater were prepared weekly to limit the potential for bacterial growth in the column feed lines. The groundwater in the feed reservoir was equilibrated with the atmosphere and therefore was air-saturated when it entered the column.

Column Design, Operation and Analyses

The experimental apparatus consisted of a 110 cm long, 10.2 cm diameter (O.D.) stainless steel column containing a 100-cm bed of column soil, underlain by a 5-cm sand layer (details of the column design are in the Supporting Information, Figure S1). Groundwater was continuously pumped through the column at a flowrate of 1.1 L/d in a downward direction. Three evenly spaced ports (Ports A, B, and C) were positioned 30, 55, and 80 cm below the top of the column, respectively, for periodic collection of 50 g (dry wt.) soil samples; less than 8% of the initial soil mass was removed from the column over the duration of the study. Nine additional smaller ports for monitoring porewater dissolved oxygen (DO) concentrations were located along the column length. Each DO port housed a dedicated stainless steel cannula, which spanned the column diameter and was screened along its length; each port was sealed with a septum and stainless-steel nut. The column was continuously operated at 20°C for eight months prior to persulfate injection ('equilibration phase') to allow for bed consolidation and inlet pressure stabilization.

The column was relocated to a 40°C constant-temperature room to initiate persulfate anion activation during persulfate injection; several studies (24,29,30) have shown that temperatures above 30°C offer significant improvement in persulfate activation and contaminant oxidation under laboratory conditions. Approximately six pore volumes of a 20 g/L persulfate solution were pumped through the column over a 16-d period, resulting in a dose of 27 mg of persulfate per g dry column soil. The selected activation temperature and persulfate dose were determined based on preliminary batch experiments (data not shown). After persulfate injection, continuous pumping of simulated groundwater was resumed in a 20°C constant-temperature room. Samples from the soil-bed surface and soil sampling ports were collected at five time points: immediately before ("pre-ox") and after (t = 0) persulfate

injection and 30, 100, and 500 d following persulfate injection. Samples were collected in 30-mL glass centrifuge vials and centrifuged for 15 min at 2,800 *g*, after which the supernatant was discarded. Aliquots of the centrifuged sample were used for PAH extraction and quantification, mineralization assays, DNA extraction and quantification, and moisture content determination.

Detailed information on PAH extraction and quantification and on mineralization assay procedures are in the Supporting Information. Briefly, aliquots of centrifuged column soil (5 g wet wt. each) were transferred to triplicate 30-mL glass centrifuge vials for solvent extraction of PAHs (using dichloromethane and acetone) and subsequent PAH quantification by high-performance liquid chromatography (HPLC). For mineralization assays, 5 g (wet wt.) of centrifuged column soil was transferred to an acid-washed 30-mL glass vial and slurried with 20 mL of sterile simulated groundwater as a source of inoculum for mineralization incubations. Assays with each sample were performed in triplicate. Each replicate consisted of a 40-mL amber EPA vial containing 1 mL of soil slurry, 4 mL of sterile simulated groundwater, a sterile glass tube containing filter paper saturated with 60 μL of 2 N KOH, and 1 μL of the radiolabelled substrate, corresponding to 20,000 disintegrations per min (dpm) for ^{14}C-acetate and 30,000 dpm for ^{14}C-phenanthrene. Triplicate killed control incubations were prepared similarly but were amended with 40 μL of phosphoric acid to decrease the pH below 2. ^{14}C-acetate was selected as a general carbon source to monitor activity of the total community (12, 26) and ^{14}C-phenanthrene was chosen to monitor phenanthrene-degrader activity.

A FOXY fiber-optic oxygen sensor system (Ocean Optics, Dunedin, FL) was used to measure DO concentrations in the column porewater (detection limit 0.1 mg/L) over the course of the experiment, except during persulfate injection. The DO sensor was inserted through a sterile hypodermic needle that was used to pierce the septum on each DO port, and it was rinsed with ethanol between measurements. Aqueous persulfate concentrations were monitored in the column effluent using a spectrophotometric method (29). Effluent pH was also periodically monitored over the course of the experiment.

Molecular Analyses

DNA was extracted in triplicate using a Qbiogene (Solon, OH) FastDNA SPIN Kit according to the manufacturer's instructions. All extractions were performed immediately following column sampling to preclude the effects of soil storage on the microbial community. The mass of DNA in each replicate was quantified with a Nanodrop™ ND-3300 fluorospectrometer (Nanodrop Technologies, Wilmington, DE) after adding Picogreen® dsDNA fluorescent indicator dye (Invitrogen; Carlsbad, CA).

Real-time quantitative PCR (qPCR) was performed to measure the abundance of total bacterial 16S rRNA genes and 16S rRNA genes from known phenanthrene-degrading bacterial groups. Primers are listed in Table S4 of the Supporting Information. Aliquots (1 μL) of pooled triplicate DNA (total volume 300 uL) from each sample were combined with the desired primers, SYBR® Green PCR master mix, and RNase-free water and run on a SmartCycler® qPCR system (Cepheid, Sunnyvale, CA) according to the manufacturer's instructions. Triplicate qPCR runs were performed for each primer set and the gene copy number was quantified only within the linear range of the respective standard curve.

Changes in microbial diversity after persulfate oxidation were monitored by DGGE as previously described (31), except a 6% polyacrylamide gel with a denaturant range of 35-65% was used for band separation and a non-denaturing stacking gel was used. A band that included members of a known PAH-degrading group, “Pyrene Group 1” (PG1) (32,33),

was identified by a separate DGGE analysis of clonal sequences phylogenetically related to this group.

To identify dominant bacterial groups before and after persulfate injection, clone libraries of 16S rRNA genes were constructed from surface soil DNA extracts from the pre-oxidation sample and 100 d post-oxidation. PCR amplification, cloning, and sequence analysis procedures are outlined in the Supporting Information. Partial 16S rRNA gene sequences recovered from this work were submitted to GenBank with accession numbers HM622160-HM622262.

Statistical Analyses

Cohen's maximum likelihood estimator method (34) was used to estimate mean and standard deviations for qPCR samples where one or more replicates were below detection. All other statistical analyses were performed using JMP® 7.0.1 (SAS Institute Inc., Cary, NC).

Results

Persulfate Breakthrough

Based on the persulfate breakthrough data (Supporting Information, Figure S2), approximately 34% of the injected persulfate mass was consumed within the column, which corresponds to an oxidant demand of 9.1 mg persulfate per g dry column soil. Batch experiments yielded a higher persulfate demand (14.5 ± 0.9 mg/g, $n = 6$) under continuously mixed, slurried conditions (data not shown). Effluent pH gradually decreased from 7.0 to 3.2 after 16 d of continuous persulfate injection but returned to neutral within approximately 60 pore volumes after persulfate was flushed from the column (data not shown).

DO Profile

Because air-saturated groundwater was continuously pumped through the column, a DO front was formed during the eight-month equilibration phase (prior to persulfate injection) that extended to Port A (Figure S3a), 30 cm below the top of the column and approximately 25 cm below the soil bed surface. Oxygen concentrations were ≤ 0.1 mg/L in the remainder of the column. Oxygen was detected throughout the column within 12 d after persulfate injection, most notably in the former anoxic region, at concentrations ranging from 2.8 to 6.9 mg/L (Figure S3b). In subsequent measurements (75, 137, 220, and 495 d post-oxidation), DO concentrations gradually decreased in this region, presumably as oxygen was consumed by the recovering community.

Microbial Activity

Pre-oxidation mineralization experiments with the surface soil revealed a community capable of mineralizing both ^{14}C-acetate and ^{14}C-phenanthrene extensively within the 15 d incubation period (75% and 60%, respectively) (Figure 1). Substantial mineralization (48-52%) of ^{14}C-acetate was also observed at Ports A, B, and C, while less than 10% of ^{14}C-phenanthrene was mineralized by samples from these ports. Immediately after persulfate injection, mineralization of both compounds was strongly inhibited at all sample locations. After 30 d, ^{14}C-acetate mineralization recovered to near pre-oxidation levels, while ^{14}C-phenanthrene mineralization remained low (<5%). Full recovery of ^{14}C-phenanthrene mineralization activity was not observed until 100 d post-oxidation in the surface soil, along with enhanced mineralization at Ports A, B, and C (where pre-oxidation activity was negligible). Since mineralization activity (for both ^{14}C-acetate and ^{14}C-phenanthrene) was restored or enhanced at all sample locations within 100 d, mineralization assays were not conducted on samples collected 500 d post-oxidation.

In supplemental batch experiments, neither an increase in temperature from 20°C to 40°C nor addition of SO_4^{2-} (which would be generated from $SO_4^{-\bullet}$ decomposition) inhibited mineralization of ^{14}C-acetate or ^{14}C-phenanthrene (data not shown).

Molecular Analyses

Clone libraries of 16S rRNA genes were constructed to identif dominant bacterial groups in DNA extracted from the surface soil before and 100 d after persulfate injection (corresponding to recovery of phenanthrene mineralization activity). A total of 109 partial 16S rRNA gene sequences were obtained from the two libraries (44 pre-oxidation and 65 post-oxidation). Six suspected chimeric sequences were excluded from further analyses. Clones were grouped at the >99% similarity level to define 13 operational taxonomic units (OTUs), with an additional 17 singleton clones. Phylogenetic relationships among the OTUs and select singleton clones are illustrated in Figure 2. A phylogenetic tree showing all sequences is provided in Supporting Information, Figure S4.

Before persulfate addition, the majority of cloned sequences (62%, 26 of 42) were associated with γ-Proteobacteria. Two of the OTUs each accounted for 31% (13 of 42) of the total clones in the pre-oxidation sample. One of these OTUs (represented by clonal sequence “pre-4”) was closely related to members of uncultivated “Pyrene Group 2” (PG2), a group of bacteria previously implicated in pyrene (32) and phenanthrene (33) degradation in a bioreactor treating a different MGP soil. The other OTU (represented by clonal sequence “pre-62”) was closely related to an uncultivated bacterial group (clonal sequence “PAH-Feed-43”) found in untreated MGP soil from an earlier study (32). Members of other known PAH-degrading groups were present, including *Acidovorax* spp. and *Sphingomonas* spp., but each were minor members of the total community.

Post-oxidation, cloned sequences were predominantly β-Proteobacteria (59%, 36 of 61). An OTU (represented by clonal sequence “post-23”) containing sequences closely related to the uncultivated clone LYC178 (GenBank entry DQ984610) from oil-contaminated soil comprised 36% (22 of 61) of the clones in the post-oxidation library. Unfortunately, no published information on Genbank entry DQ984610 is available for comparative purposes. Sequences related to PG1 (represented by clonal sequence “post-66”), another uncultivated group of organisms associated with pyrene (32) and phenanthrene (33) degradation, comprised 11% (7 of 61) of the post-oxidation clone library. The dominant members of the pre-oxidation library appeared adversely affected by the addition of persulfate. The relative abundance of clones related to clone PAH-Feed-43 decreased from 31% (13 of 42) to 15% (9 of 61) in the post-oxidation community, while no clones related to PG2 were recovered. Other genera associated with PAH degradation were identified in low abundances 100 d after persulfate injection, including members of the *Sphingomonas*, *Novosphingobium*, and *Ralstonia* genera.

The 16S rRNA gene copy numbers of total bacteria and groups PG1 and PG2 were tracked for all sample locations and time points by qPCR. Pre-oxidation, total bacterial abundance was greatest at the soil-bed surface ($6.2 \pm 2.4 \times 10^8$ genes/g dry soil) and declined with depth (Figure 3). Following persulfate injection, a two- to three-log reduction in total bacteria was observed at all sample locations, with surface soil abundance below the detection limit of 3×10^5 genes/g. By 30 d post-oxidation, the bacterial community had recovered substantially, approaching pre-oxidation levels (10^7-10^8 genes/g) at all sample locations. Quantification of DNA mass yielded a similar recovery pattern within 30 d post-oxidation (data not shown).

The 16S rRNA genes associated with the known PAH-degrading groups PG1 and PG2 were most abundant in the upper section of the column pre-oxidation, with surface soil

concentrations of $7.6 \pm 0.7 \times 10^7$ and $1.2 \pm 0.2 \times 10^8$ genes/g, respectively (Figure 3). Group PG2 sequences were more abundant at Ports A and B than were group PG1 sequences. Immediately following persulfate injection, PG1 and PG2 sequences were not detected at any sample location and remained below detection at 30 d, even though recovery of total bacteria had been established. Recovery of PG1 organisms was first observed at 100 d post-oxidation in the surface soil and at Ports A and B, with concentrations above the respective pre-oxidation levels, and they were eventually detected at Port C 500 d post-oxidation. Group PG2 organisms required additional time to re-establish, achieving near pre-oxidation levels or greater at all sample locations by 500 d post-oxidation.

Microbial community profiles as determined by DGGE analysis of 16S rRNA genes are illustrated in Figure 4. Clear differences in the pre-oxidation community (lanes 1-4) were observed over the column depth. Consistent with the data shown in Figure 3, the intensity of the DGGE band associated with group PG1 decreased between the surface and Port A, and was not observed at Ports B and C. It was not possible to identify a single band associated with group PG2 because sequence variations among PG2-related clones resulted in two distinct DGGE bands (not shown). The transitional community observed at Port A (Figure 4, lane 2) coincided with the boundary of the pre-oxidation DO front (Figure S3a). Immediately after persulfate injection, DGGE profiles (Figure 4, lanes 5-8) were similar with depth but appeared less diverse than in the pre-oxidation samples, exhibiting only a few strong bands. At 30 and 100 d post-oxidation, community diversity increased and some differences among sample locations were re-established. Of particular note was the rebound of group PG1 in the surface soil and at Port A (Figure 4, lanes 13 and 14) and its appearance at Port B (lane 15), which corresponds well with qPCR results (Figure 3a).

Soil PAH Concentration

Significant reductions ($p < 0.05$) in PAH concentrations (mainly three- and four-ring PAHs) were observed at the surface soil (59% of total PAHs) and Port A (26% of total PAHs) during the column equilibration phase, as a result of continuous dissolution and aerobic biodegradation within the DO front (Figure S5). Phenanthrene concentrations decreased by 74% and 28% in the surface soil and at Port A, respectively, although the reduction was not statistically significant ($p > 0.05$) at Port A. No significant differences ($p > 0.05$) in PAH concentrations were noted at Ports B and C (within the anoxic zone of the column). The injection of persulfate, however, had little impact on PAH concentrations at all sample locations, with only acenaphthene and anthracene (at Port B) exhibiting significant reductions in concentration after the persulfate injection period (Figure S5). This observation is in contrast to the results of batch efficacy tests, in which up to 47% of total PAHs were removed after 16 d of persulfate treatment at 40°C (Figure S6). Phenanthrene concentrations were not statistically different ($p > 0.05$) pre- and post-oxidation at all sample locations (Figure S5).

Discussion

Exposure to persulfate had a major impact on the total microbial community in the column soil, as evidenced by a two- to three-log reduction in total bacterial abundance, inhibition of ^{14}C-acetate mineralization, and a decrease in community diversity after injection. However, this adverse effect was short-lived, with near-complete recovery (both in bacterial 16S rRNA gene abundance and acetate-mineralization activity) observed at all sample locations within 30 d after persulfate exposure. Chapelle et al. (12) reported similar results in a field-scale application of Fenton's reagent, where bacterial counts and ^{14}C-acetate mineralization declined and subsequently recovered within six months of oxidant injection. Other microbial exposure studies with Fenton's reagent (9,10), permanganate (14), ozone (35), and steam injection (5) reported substantial reductions in bacterial counts with

moderate to complete recovery following treatment. Explanations for the observed microbial recovery (3,4,36) have included improved bioavailability of intermediate substrates from the oxidation of contaminants or SOM; introduction of new organisms from upgradient groundwater; reduced contaminant concentrations below toxic levels; die-off of microbial predators; and/or the generation of terminal electron acceptors. Preferential flow pathways and the presence of microbial microniches in heterogeneous soils can also limit direct contact between the oxidant and microbes, allowing microbial survival under harsh oxidative conditions (3). In contrast to our results, Tsitonaki et al. (26) found little effect of heat-activated persulfate (0.02-2 g/kg) on cell density, with reductions in ^{14}C-acetate mineralization activity observed only at the highest persulfate dose. The decrease in activity was attributed to a drop in pH following persulfate addition, which may have interfered with acetate metabolism. Persulfate doses used in their work were also much lower (one to three orders of magnitude) than in this study, which might explain the differences in microbial response to persulfate exposure.

Phenanthrene mineralization activity and the abundances of known PAH-degrading bacterial groups, PG1 and PG2, were greatly impacted by persulfate exposure, requiring additional time to recover in comparison to the overall microbial community. This lag in recovery might reflect lower initial PG1 and PG2 concentrations in the pre-oxidation community, resulting in quicker recovery for those bacterial groups with larger initial populations. However, the fact that PG1 and PG2 organisms recovered at different times (despite having similar initial abundances in the surface soil) suggests that recovery time might also be a function of group-specific tolerance (or degree of sensitivity) to oxidative conditions and radical exposure.

Effects of Oxygen on the Microbial Community

Establishment of a DO front in the upper section of the column (due to continuous influx of air-saturated groundwater) appeared to influence community diversity with depth in the pre-oxidation soil, as evidenced by variations in DGGE banding patterns (Figure 4) and a decrease in PG1 and PG2 sequence abundance with depth (Figure 3). After persulfate injection, oxygen detected in the former anoxic region of the column (Figure S3b) may be attributed to persulfate decomposition and/or a decrease in oxygen demand due to microbial inactivation. The formation or penetration of oxygen may have helped stimulate post-oxidation recovery of groups PG1 and PG2, although variations in time between soil sampling events and DO measurements make it difficult to pinpoint this effect.

PAH Removal

The lack of PAH removal observed after persulfate injection may be attributed to reduced PAH availability compared to the preliminary, continuously mixed batch experiments. The availability of PAHs may have been particularly low in the surface soil and Port A as a result of continuous dissolution and aerobic biodegradation of the most readily available fraction of the PAHs during the eight-month equilibration phase. An earlier study (22) found that persulfate was capable of oxidizing only the bioavailable fraction of PAHs in a variety of field-contaminated soils and sediments. These findings call into question the applicability of persulfate for the oxidation of highly weathered contaminants, as typically encountered at former MGP sites.

Implications for Field Applications

This study has illustrated that persulfate oxidation is compatible with subsequent bioremediation with respect to recovery of the overall microbial community and, more importantly, specific PAH-degrading bacterial groups in the soil matrix. A key finding was that complete recovery of phenanthrene-degrading bacteria took longer relative to the

overall community, suggesting that rates of recovery of individual bacterial species are not equivalent. Differences in initial abundance, oxidative-stress resistance, and availability of preferred substrate and/or electron acceptors can impact microbial recovery, and hence diversity, post-oxidation. In terms of field application, these results suggest that the quantity or activity of total bacteria may be inappropriate as a surrogate measure of contaminant degrader recovery. Previous studies investigating coupled chemical-biological treatment have, in general, overlooked the effects of oxidation on specific contaminant-degrading bacteria.

Supplementary Material

Refer to Web version on PubMed Central for supplementary material.

Acknowledgments

We thank Randall Goodman and Glenn Walters for their help in the design and construction of the column apparatus and David Singleton for the reverse primer for group PG2. We also thank Maiysha Jones and David Singleton for their invaluable advice on molecular techniques. This work was supported by the National Institute of Environmental Health Sciences (grant number 5 P42 ES005948).

Literature Cited

1. Azadpour-Keeley A, Wood LA, Lee TR, Mravik SC. Microbial responses to *in situ* chemical oxidation, six-phase heating, and steam injection remediation technologies in groundwater. Remediation J. 2004; 14:5–17.
2. Hrapovic L, Sleep BE, Major DJ, Hood ED. Laboratory study of treatment of trichloroethene by chemical oxidation followed by bioremediation. Environ. Sci. Technol. 2005; 39:2888–2897. [PubMed: 15884390]
3. Huling, SG.; Pivetz, BE. In-Situ Chemical Oxidation. U.S. Environmental Protection Agency; Cincinnati OH: 2006. Engineering Issue Paper, EPA 600-R-06-072
4. Sahl J, Munakata-Marr J. The effects of *in situ* chemical oxidation on microbiological processes: A review. Remediation J. 2006; 16:57–70.
5. Richardson RE, James CA, Bhupathiraju VK, Alvarez-Cohen L. Microbial activity in soils following steam treatment. Biodegradation. 2002; 13:285–295. [PubMed: 12521292]
6. Siegrist, RL.; Urynowicz, MA.; West, OR.; Crimi, ML.; Lowe, KS. Principles and Practices of In Situ Chemical Oxidation Using Permanganate. Battelle Press; Columbus: 2001. p. 348
7. Imlay JA, Linn S. DNA damage and oxygen radical toxicity. Science. 1988; 240:1302–1309. [PubMed: 3287616]
8. Büyüksönmez F, Hess TF, Crawford RL, Watts RJ. Toxic effects of modified Fenton reactions on *Xanthobacter flavus* FB71. Appl. Environ. Microbiol. 1998; 64:3759–3764. [PubMed: 9758796]
9. Stokley, KE.; Drake, EN.; Prince, RC. The role of Fenton's reagent in soil bioremediation.. In situ and On-site Bioremediation; Proceeding of the Fourth International Conference; New Orleans, USA. April 28-May 1; 1997. p. 487-492.
10. Kastner JR, Domingo JS, Denham M, Molina M, Brigmon RL. Effect of chemical oxidation on subsurface microbiology and trichloroethene (TCE) biodegradation. Bioremediation J. 2000; 4:219–236.
11. Allen, SA.; Reardon, KF. Remediation of contaminated soils by combined chemical and biological treatments.. In: Wickramanayake, GB.; Gavaskar, AR., editors. Physical and Thermal Technologies, Proceedings of the Second International Conference on Remediation of Chlorinated and Recalcitrant Compounds; Monterey, USA. May 22-25, 2000; Columbus, OH: Battelle Press; 2000.
12. Chapelle FH, Bradley PM, Casey CC. Behavior of a chlorinated ethene plume following source-area treatment with Fenton's reagent. Ground Water Monit. Rem. 2005; 25:131–141.

13. Palmroth M, Langwaldt J, Aunola T, Goi A, Munster U, Puhakka J, Tuhkanen T. Effect of modified Fenton's reaction on microbial activity and removal of PAHs in creosote oil contaminated soil. Biodegradation. 2006; 17:29–39.

14. Klens, J.; Pohlmann, D.; Scarborough, S.; Graves, D. The effects of permanganate oxidation on subsurface microbial populations.. In: Leeson, A.; Kelley, ME.; Rifai, HS.; Maar, VS., editors. Natural Attenuation of Environmental Contaminants, Proceedings of the Sixth International In Situ and On-Site Bioremediation Symposium; San Diego, USA. June 4-7, 2001; Columbus, OH: Battelle Press; 2001.

15. Rowland, MA.; Brubaker, GR.; Kohler, K.; Westray, M.; Morris, D. Effects of potassium permanganate oxidation on subsurface microbial activity.. In: Magar, VS.; Fennel, DE.; Morse, JJ.; Alleman, BC.; Leeson, A., editors. Anaerobic Degradation of Chlorinated Solvents, Proceedings of the Sixth International In Situ and On-Site Bioremediation Symposium; San Diego, USA. June 4-7, 2001; Columbus, OH: Battelle; 2001.

16. Sahl JW, Munakata-Marr J, Crimi ML, Siegrist RL. Coupling permanganate oxidation with microbial dechlorination of tetrachloroethene. Water Environ. Res. 2007; 79:5–12. [PubMed: 17290967]

17. Watts RJ, Teel AL. Treatment of contaminated soils and groundwater using ISCO. Pract. Periodical of Haz. Toxic and Radioactive Waste Mgmt. 2006; 10:2–9.

18. Bartlett PD, Cotman JD. The kinetics of the decomposition of potassium persulfate in aqueous solutions of methanol. J. Am. Chem. Soc. 1949; 71:1419–1422.

19. Kolthoff IM, Miller IK. The chemistry of persulfate. I. The kinetics and mechanism of the decomposition of the persulfate ion in aqueous medium. J. Am. Chem. Soc. 1951; 73:3055–3059.

20. House DA. Kinetics and mechanism of oxidations by peroxydisulfate. Chem. Rev. 1962; 62:185–203.

21. Peyton, GR.; LeFaivre, MH.; Smith, MA. Treatability of contaminated ground water and aquifer solids at town gas sites, using photolytic ozonation and chemical in-situ reclamation. Hazardous Water Research and Information Center, Illinois State Water Survey Division; Savoy, IL: 1990. HWRIC-RR-048

22. Cuypers C, Grotenhuis JTC, Joziasse J, Rulkens WH. Rapid persulfate oxidation predicts PAH bioavailability in soils and sediments. Environ. Sci. Technol. 2000; 34:2057–2063.

23. Nadim F, Huang KC, Dahmani A. Remediation of soil and ground water contaminated with PAH using heat and Fe(II)-EDTA catalyzed persulfate oxidation. Wat. Air Soil Pollut. Focus. 2006; 6:227–232.

24. Waldemer RH, Tratnyek PG, Johnson RL, Nurmi JT. Oxidation of chlorinated ethenes by heat-activated persulfate: Kinetics and products. Environ. Sci. Technol. 2007; 41:1010–1015. [PubMed: 17328217]

25. Johnson RL, Tratnyek PG, Johnson RO. Persulfate persistence under thermal activation conditions. Environ. Sci. Technol. 2008; 42:9350–9356. [PubMed: 19174915]

26. Tsitonaki A, Smets BF, Bjerg PL. Effects of heat-activated persulfate oxidation on soil microorganisms. Water Res. 2008; 42:1013–1022. [PubMed: 17942135]

27. Lukasewycz MT, Burkhard LP. Complete elimination of carbonates: A critical step in the accurate measurement of organic and black carbon in sediments. Environ. Toxicol. Chem. 2005; 24:2218–2221. [PubMed: 16193748]

28. Groves, MR. Preliminary Report on Groundwater Resources in Rowan County. North Carolina Department of Natural and Economic Resources; North Carolina: 1976.

29. Huang KC, Couttenye RA, Hoag GE. Kinetics of heat-assisted persulfate oxidation of methyl tert-butyl ether (MTBE). Chemosphere. 2002; 49:413–420. [PubMed: 12365838]

30. Liang C, Bruell CJ, Marley MC, Sperry KL. Thermally activated persulfate oxidation of trichloroethylene (TCE) and 1,1,1-trichloroethane (TCA) in aqueous systems and soil slurries. Soil Sed. Contam. 2003; 12:207–228.

31. Singleton D, Richardson S, Aitken M. Effects of enrichment with phthalate on polycyclic aromatic hydrocarbon biodegradation in contaminated soil. Biodegradation. 2008; 19:577–587. [PubMed: 17990065]

32. Singleton DR, Powell SN, Sangaiah R, Gold A, Ball LM, Aitken MD. Stable-isotope probing of bacteria capable of degrading salicylate, naphthalene, or phenanthrene in a bioreactor treating contaminated soil. Appl. Environ. Microbiol. 2005; 71:1202–1209. [PubMed: 15746319]

33. Singleton DR, Hunt M, Powell SN, Frontera-Suau R, Aitken MD. Stable-isotope probing with multiple growth substrates to determine substrate specificity of uncultivated bacteria. J. Microbiol. Methods. 2007; 69:180–187. [PubMed: 17267058]

34. Cohen AC Jr. Simplified estimators for the normal distribution when samples are singly censored or truncated. Technometrics. 1959; 1:217–237.

35. Jung H, Ahn Y, Choi H, Kim IS. Effects of in-situ ozonation on indigenous microorganisms in diesel contaminated soil: Survival and regrowth. Chemosphere. 2005; 61:923–932. [PubMed: 16257315]

36. Tsitonaki A, Petri B, Crimi M, Mosbaek H, Siegrist RL, Bjerg PL. In situ chemical oxidation of contaminated soil and groundwater using persulfate: A review. Crit. Rev. Environ. Sci. Technol. 2010; 40:55.

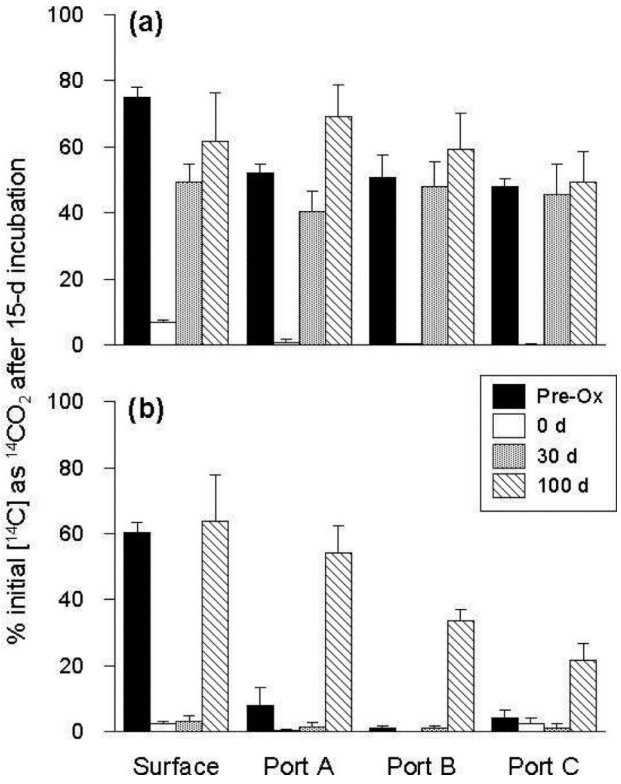

Figure 1.

Mineralization of ^{14}C-acetate (a) and ^{14}C-phenanthrene (b) by the soil microbial community at each column sampling location before persulfate injection (“pre-ox”), immediately after injection (0 d) and 30 and 100 d post-injection. Values represent the means and standard deviations of triplicate 15-d incubations.

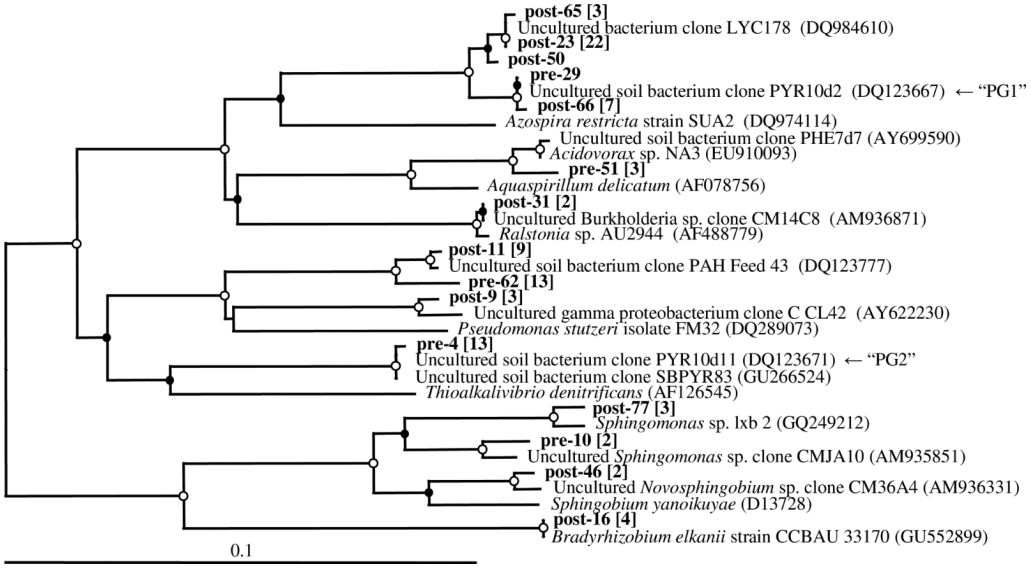

Figure 2.

Neighbor-joining phylogenetic tree of 16S rRNA gene sequences recovered pre- and post-oxidation (100 d) from the column surface soil and selected close relatives. Clones from this study (in bold) follow the naming scheme of "pre" (pre-oxidation) and "post" plus an assigned number for identification purposes. Square brackets (in bold) include the number of sequences within an OTU represented by the clonal sequence shown. GenBank accession numbers are shown in parentheses for the selected reference sequences. Bootstrap values are indicated on nodes with an open (○) and closed (●) circle representing ≥95 and ≥50% bootstrap support, respectively. *Thermus aquaticus* YT-1 (L09663) was used as an outgroup (not shown). Sequences associated with groups PG1 and PG2 are indicated with an arrow.

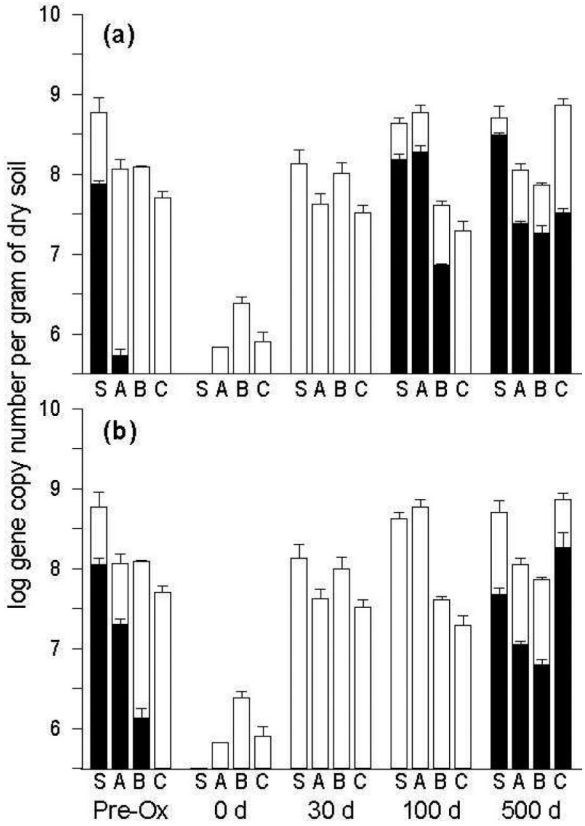

Figure 3.

Abundance of 16S rRNA gene sequences representing groups PG1 (a) and PG2 (b) in the column soil pre- and post-oxidation (black bars), relative to total bacterial abundance (white bars). Values represent the log-transformed mean and standard deviation of triplicate qPCR runs of pooled DNA extracts. The minimum value on the y-axis is the average quantification limit for all primer sets (3×10^5 genes/g). Samples from the soil bed surface and column sampling ports are designated S, A, B and C, respectively.

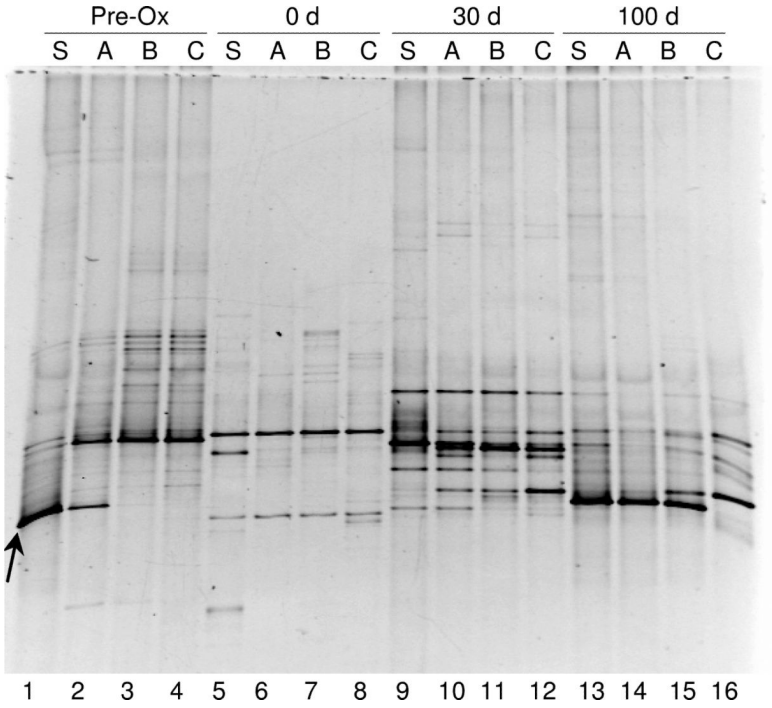

Figure 4.
Negative image of DGGE gel delineating 16S rRNA genes pre- and post-oxidation (0, 30, and 100 d) at the surface soil (S) and ports A, B, and C. Gel lanes were arranged according to column depth for each time point as follows: pre-oxidation (lanes 1-4), immediately post-oxidation (lanes 5-8), 30 d post-oxidation (lanes 9-12) and 100 d post-oxidation (lanes 13-16). The location of the band corresponding to group PG1 sequences is indicated with an arrow.